Strojniški vestnik - Journal of Mechanical Engineering 56(2010)10, 625-636
UDC 539.61
Paper received: 20.08.2009
Paper accepted: 19.07.2010

Strength and Fracture Strain of Resin/filler Systems Using Two Models (1) of Perfect and (2) of Low Adhesion Quality

George Bourkas, Emilios Sideridis, Christos Younis, Ioannis N. Prassianakis*, Victor Kitopoulos
Faculty of Applied Mathematical and Physical Sciences, Department of Mechanics, Laboratory of Testing and Materials, National Technical University of Athens – Zografou Campus, Greece

The tensile strength and the fracture strain of particulate composites have been evaluated for the case that adhesion exists between the matrix and filler. Two models, each of three components on the basis of cube-within-cube formation, have been used as representative volume elements. By comparing the derived theoretical results of the strength with experimental data for treated and untreated particles in resin/filler systems, the first model can be characterised as corresponding to perfect adhesion quality between the matrix and filler, while the second one to low adhesion quality. The strength predicted by the first model is close to that of treated particles corresponding to high strength. This model corresponds to an upper bound of the strength in cube-within-cube models. The strength predicted by the second model is close to that of untreated particles corresponding to low strength, but this model does not correspond to a lower bound of strength. The systems used for comparison were resin/glass, resin/iron and resin/SiC particulate composites. For the case that adhesion exists between the matrix and filler, the strengths and fracture strains predicted by the present models are in agreement to those provided by an existing evaluation method in the literature.

Keywords: resin/filler systems, microstructure, fracture strain, perfect adhesion quality, low adhesion quality

0 INTRODUCTION

As pointed out by Nielsen [1], when there is no adhesion between matrix and filler, the tensile strength of particulate composites depends on the tensile strength of the matrix, the filler volume fraction and the stress concentration factor. When adhesion between the matrix and filler exists, the tensile strength depends on the fracture deformation and the elastic modulus of the composite. Consequently, in this latter case the tensile strength results from a complex interplay between the properties of the individual constituent phases; the resin, the filler and the interface [2].

In general, when adhesion exists between the matrix and filler, the mechanical properties of the composite are affected by a number of parameters; the size, the shape, the aspect ratio (ratio of the length to the side of the base), the distribution of the reinforcing particles, the interaction between the inclusions and the agglomerations of fillers. In the case of nonspherical inclusions the orientations of the fillers with respect to the applied stress are also essential [2]. Some significant parameters also play an important role upon the tensile strength; the quality of adhesion between the matrix and filler, air bubbles in the matrix, the stress concentration factor, the plastic behavior of the matrix near the filler and the crack pinning effect (that is when the crack propagation is embedded by a group of particles) [2] and [3].

In [4] and [5], tensile experiments in particulate composites prepared by treated and untreated particles, have shown that the adhesion quality between the matrix and filler considerably affects the strength behavior of the composites. The kind of adhesion also affects the values of the stress intensity factor [3] and [6].

In this study the tensile strength and the fracture strain of particulate composites are evaluated using two cube-within-cube models, each one consisting of three components. One of these models [7] gives a constant strength of the composite, independent of the filler content, which is equal to the strength of the matrix. Thus, this model is characterized as corresponding to

*Corr. Author's Address: Faculty of Applied Mathematical and Physical Sciences, Depart. of Mechanics, National Tech. University of Athens – Zografou Campus, GR – 15773, Athens, Greece, prasian@central.ntua.gr

perfect adhesion quality between the matrix and filler. In the other model [8] the strength decreases as the filler content increases up to 20%, attains a minimum and then increases steadily with a slow rate. A comparison to experimental results [4] and [5] shows that this model corresponds to low adhesion quality between the matrix and filler. The strength and fracture strain predicted by the above models are in agreement with the theory of Nielsen [1] for the case when adhesion exists between the matrix and filler. The theoretical results derived by the presented models are compared to the values of the strength predicted by existing equations in the literature and to experimental results in resin/glass particulate composites. A comparison of the theoretical values of strength and fracture strain is also made with experimental results in resin/iron and resin/SiC particulate composites.

1 THEORETICAL CONSIDERATIONS

The theoretical analysis is based on the following assumptions:

1) The particles are perfectly cubic.
2) The matrix volume distribution of each filler is also cubic.
3) The volume fraction of the particles is sufficiently low, so that there is no interaction between the stress fields around the neighboring particles.
4) The particles are uniformly distributed in the matrix, so that homogeneity can be assumed.
5) Both the matrix and the inclusion are prepared from perfectly homogeneous, elastic and isotropic materials of known mechanical properties.
6) The matrix is brittle and the stress-strain linearity is maintained up to the failure of the composite.
7) There is no transverse variation of the strains in the components which are connected in parallel and have the same length in the load direction.
8) The stresses do not vary in the direction of the applied load in the components which are connected in a series and have the same cross sections.

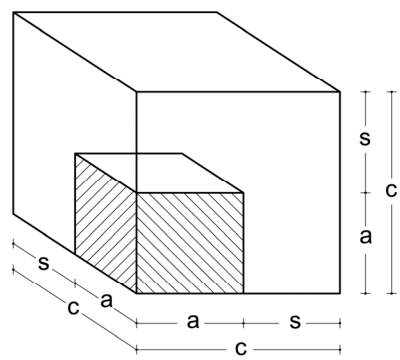

Fig. 1. *A schematic representation of the cube-within-cube model*

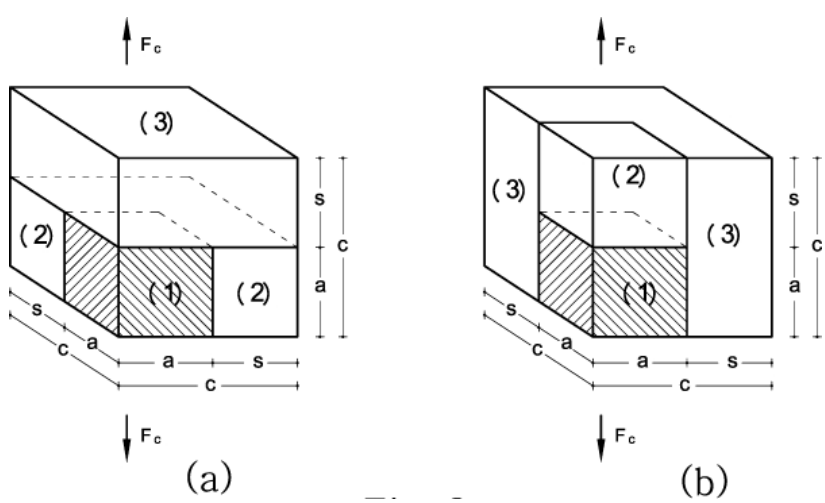

Fig. 2. *The two cube-within-cube models each consisting of three components, a) Paul's model [7], b) Ishai-Cohen's model [8]*

As shown in Fig. 1 the filler volume fraction is given by:

$$u_f = a^3 / c^3 . \quad (1)$$

The components (1) and (2) of the model presented in Fig. 2a, called model 1, are connected in parallel and the resulting element is connected in a series with a component (3).

When an external force acts in the direction shown in Fig. 2a the stress equilibrium and strain compatibility equations are:

$$\sigma_3 = \sigma_c , \quad (2)$$

$$\sigma_c = \sigma_1 u_f^{2/3} + \sigma_2 (1 - u_f^{2/3}) , \quad (3)$$

$$\varepsilon_1 = \varepsilon_2 , \quad (4)$$

$$\varepsilon_c = \varepsilon_1 u_f^{1/3} + \varepsilon_3 (1 - u_f^{1/3}) , \quad (5)$$

where the indexes 1, 2 and 3 correspond to the components (1), (2), (3) and the composite respectively. The constitutive equations are:

$$\sigma_1 = \varepsilon_1 \mathrm{E_f} , \quad (6)$$

$$\sigma_2 = \varepsilon_2 \mathrm{E_m} , \quad (7)$$

$$\sigma_3 = \varepsilon_3 \mathrm{E_m} , \quad (8)$$

$$\sigma_c = \varepsilon_c \mathrm{E_c} , \quad (9)$$

where the indexes correspond to the matrix and the filler respectively.

Combining Eqs. (2) to (9) one obtains:

$$\sigma_1 > \sigma_3 = \sigma_c > \sigma_2 . \quad (10)$$

Assuming that failure in the component (3) corresponds to failure of the whole composite, the strength of the whole composite is given by:

$$\sigma_{cu} = \sigma_{mu} , \quad (11)$$

where the index denotes strength.

Eqs. (2) to (9) give:

$$\varepsilon_{cu} = \varepsilon_{mu} \left[1 - u_f^{1/3} \left(1 - \frac{1}{(m-1) u_f^{2/3} + 1} \right) \right] , \quad (12)$$

where the index u denotes fracture deformation and $m = E_f / E_m$.

On the other hand, in the model presented in Fig. 2b, called model 2, the components (1) and (2) are connected in a series and the resulting element is connected in parallel with component (3). When a load acts in the direction shown in Fig. 2b the governing stress-strain equations are:

$$\sigma_c = \sigma_1 u_f^{2/3} + \sigma_3 (1 - u_f^{2/3}) , \quad (13)$$

$$\sigma_1 = \sigma_2 , \quad (14)$$

$$\varepsilon_3 = \varepsilon_c , \quad (15)$$

$$\varepsilon_c = \varepsilon_1 u_f^{1/3} + \varepsilon_2 (1 - u_f^{1/3}) . \quad (16)$$

The constitutive relations are given by Eqs. (6) to (9). Combining Eqs. (6) to (9) with Eqs. (13) to (16) it follows that:

$$\sigma_1 = \sigma_2 > \sigma_c > \sigma_3 . \quad (17)$$

Assuming that failure of the composite coincides with failure of the component (2), Eqs. (6) to (9) and (13) to (16) give

$$\sigma_{cu} = \sigma_{mu} \left[1 - (u_f^{1/3} - u_f) \frac{m-1}{m} \right] \quad (18)$$

and

$$\varepsilon_{cu} = \varepsilon_{mu} \left[1 - \frac{m-1}{m} u_f^{1/3} \right] , \quad (19)$$

where $m = E_f / E_m$.

Alternatively, in both models (1) and (2) strength can also be given by the relation:

$$\sigma_{cu} = \varepsilon_{cu} E_c , \quad (20)$$

where the elastic modulus derived by model (1) is given [7] by:

$$E_c = E_m \left(\frac{1 + (m-1) u_f^{2/3}}{1 + (m-1)(u_f^{2/3} - u_f)} \right) , \quad (21)$$

while the elastic modulus derived by model (2) is given [8] by:

$$E_c = E_m \left(1 + \frac{u_f}{\frac{m}{m-1} - u_f^{1/3}} \right) . \quad (22)$$

To take into account the effect of the matrix volume distribution of each filler on the values of the fracture constants, the models 3 and 4 are introduced, shown in Figs. 3a and 3b, respectively.

Following a similar procedure to that presented for models 1 and 2, model 3 gives:

$$\sigma_{cu} = \sigma_{mu} , \quad (23)$$

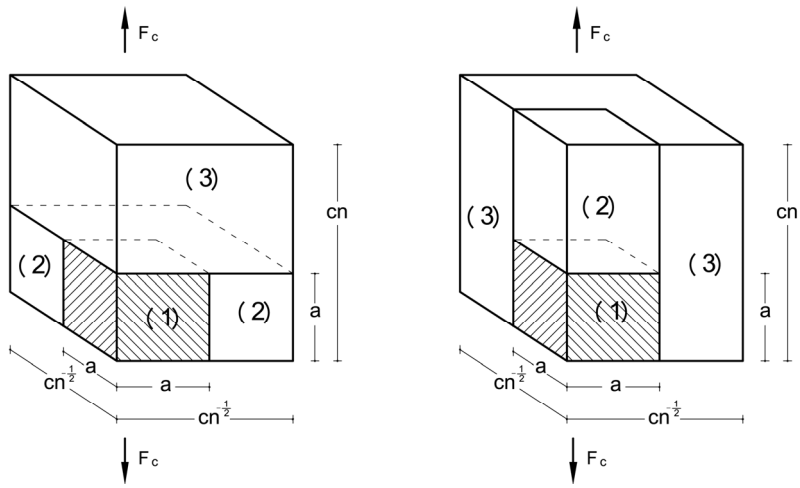

a) *b)*

Fig. 3. *The two cube-within-prisma parametric models consisting of three components (models 3 and 4 respectively)*

$$\varepsilon_{cu} = \varepsilon_{mu}\left\{1 - u_f^{1/3}\left[\frac{u_f^{2/3}(m-1)}{u_f^{2/3} n (m-1)+1}\right]\right\} \tag{24}$$

and

$$E_c = E_m\left(1 + \frac{u_f}{\frac{1}{m-1} + u_f^{2/3}\, n^{-1} - u_f}\right). \tag{25}$$

Similarly for Model 4 the following is obtained:

$$\sigma_{cu} = \sigma_{mu}\left[1 - \left(u_f^{1/3}\, n^{-1} - u_f\right)\frac{m-1}{m}\right], \tag{26}$$

$$\varepsilon_{cu} = \varepsilon_{mu}\left(1 - \frac{u_f^{1/3}(m-1)}{m\, n}\right) \tag{27}$$

and

$$E_c = E_m\left(1 + \frac{u_f}{\frac{m}{m-1} - u_f^{1/3}\, n}\right). \tag{28}$$

Using Eqs. (23) to (28) the effect of inhomogeneous distribution of the fillers into the volume of the matrix can be estimated.

2 MATERIALS AND EXPERIMENTAL WORK

The first material used in the present work was derived from a basic diglycidyl ether of bisphenol-A resin epoxy matrix with an epoxy equivalent of 185 to 192 m mol/kg, a molecular mass between 370 and 384 and a viscosity of 15 Ns/m^2 at 25°C. A curing agent, 8 p.h.r. by weight triethylenetetramine was employed. This material was filled with iron particles of average radius 75 μm. The elastic moduli of the matrix and filler were 3.50 and 210 GPa respectively, their Poisson ratio were 0.35 and 0.29 respectively and the densities were 7800 and 1190 kg/m^3 , respectively. The volume fraction was 0, 0.05, 0.1, 0.15, 0.2, 0.25, 0.3, and 0.4.

The second material consisted of an epoxy resin with a viscosity of 10 to 12 Ns/m^2 at 25 °C and an epoxy equivalent of 5340 to 5500 m mol/kg and density of 1160 kg/m^3. The used hardener was Epilink 177 with an equivalent of ~95 and viscosity between 0.25 and 0.70 Ns/m^2 at 25 °C. The rate of mixture with the resin was 50 p.h.r. Also, a plasticizer D.O.P. at a rate of 35 p.h.r. was employed.

A filler SiC particles of an average radius of 46 μm was used. The elastic modulus, the Poisson ratio and the density of the filler were 400 GPa, 0.2 and 3170 kg/m^3 , respectively. The elastic modulus and the Poisson ratio of the system matrix-hardener-plasticizer were determined from the experiments as 2.20 and 0.39 GPa, respectively. The volume fraction of this material was 0, 0.05, 0.1, 0.2 and 0.3.

In order to measure ultimate stress, fracture strain and the Elastic modulus of the materials, tensile experiments were carried out with an Instron-type testing machine at room

temperature. Specimens were tested at a rate of extension of 0.2 mm/sec. The specimens were of dog-bone type with dimensions at a measuring area of $50 \cdot 10^{-3} \times 20 \cdot 10^{-3} \times 9 \cdot 10^{-3}$ m^3 and of total length $150 \cdot 10^{-3}$ m. In order to obtain the stress-strain diagrams for each material, strain gauges (KYOWA type, gauge factor k = 1.99) were located on each specimen to measure the strain.

3 RESULTS AND DISCUSSION

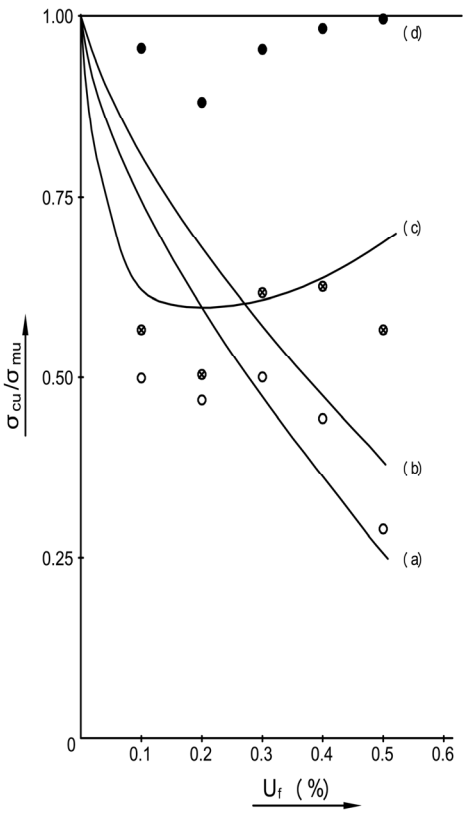

Fig. 4. *Ratio $\sigma_{cu} / \sigma_{mu}$ (strength of the composite over strength of the matrix) as a function of the volume fraction filler u_f 4.5 μm particles: • treated with A187; ⊗ untreated; ∘ DC 1107 treated (after Spanoudakis and Young), (a) Nikolais and Narkis, Eq. (34), (b) B. Nielsen, Eq. (33), (c) model 2; (d) model 1*

In Figs. 4 and 5 the tensile strength in resin/glass particulate composites versus the filler content is plotted. The strength predicted by Eqs. (18) and (11) corresponds to the curves (c) and (d), respectively. In the same figures the theoretical values of the strength derived by Eqs. (33) and (34) (Appendix 1) are also shown. The experimental results come from [4] and [5] of Spanoudakis and Young for the following cases:

1. treated particles with an improvement of the adhesion quality between matrix and filler,
2. untreated particles, and
3. treated particles with a result in a way that there is no adhesion between matrix and filler.

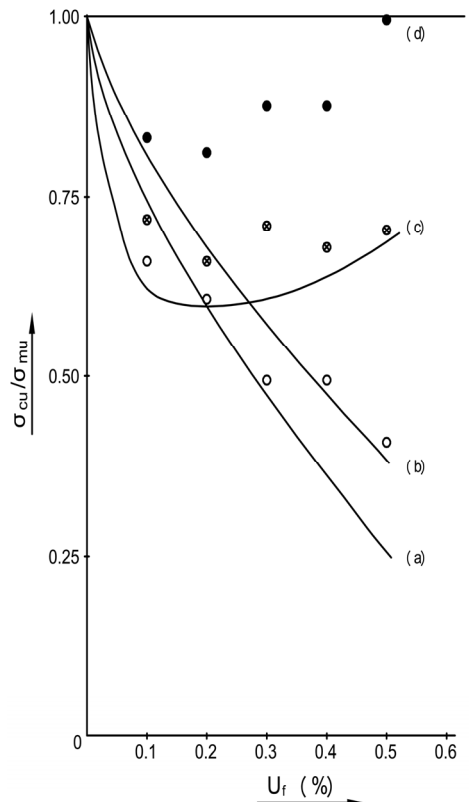

Fig. 5. *Ratio $\sigma_{cu} / \sigma_{mu}$ as a function of the volume fraction filler u_f 62 μm particles; • treated with A187, ⊗ untreated; ∘ DC 1107 treated (after Spanoudakis and Young); (a) Nikolais and Narkis, Eq. (34); (b) B. Nielsen, Eq. (33); (c) model 2; (d) model 1*

From Figs. 4 and 5 it is observed that the straight line which corresponds to model 1, curve (d), is close to the experimental results of treated glass particles with an improved adhesion between matrix and filler. The observed discrepancies are owed to the fact that the adhesion in the specimens is not perfect and due to too many parameters which affect the strength and which are referred to in the Introduction. For

the above reasons Model 1 is characterized as corresponding to perfect adhesion quality between the matrix and filler.

From the above Figs. 4 and 5 it is also observed that the strength derived by Model 2 is close to the experimental curve corresponding to the lower values of untreated particles. Thus, Model 2 corresponds to low adhesion quality between matrix and filler. This model does not consist of a lower bound of the strength because there can be models with the same geometry of the components but with different dimensions that give lower values of the strength. In the case of Model 2 failure of the component (2) causes failure of the whole composite in which the local stress concentration factor is given by:

$$\sigma_3^{'} = k\left[\sigma_{mu}\frac{m(1-u_f^{1/3})+u_f^{1/3}}{m}+\sigma_{mu}\frac{u_f^{2/3}}{1-u_f^{2/3}}\right] > \sigma_{mu}\,. \tag{29}$$

The first term in the brackets is the stress in component (3), when failure takes place in component (2). The second term in the brackets is the stress in component (2) which is now transferred to component (3). The above procedure is based on the assumption that the stresses can be transferred to the inclusion through component (2).

From the above expression the values of the stress concentration factor k, for different values of the filler volume fraction u_f in resin/iron particulate composites are given in Table 1.

Table 1. *Stress concentration factor k versus filler volume fraction* u_f

u_f	0.05	0.10	0.15	0.20	0.25
k	1.26	1.21	1.13	1.05	0.94

The above values of k determine if failure of component (2) causes failure of the whole composite.

In Figs. 6 to 9 the ratio of the strength of the composite to the strength of the matrix is plotted, versus the filler volume fraction in resin/iron composites (Figs. 6 to 8) and in resin/SiC particulate composites (Fig. 9). In the same figures the theoretical results derived from Eqs. (33) and (34) (Appendix 1) and by the models 1 and 2 are also presented. Especially in Figs. 7 and 8, the theoretical curves derived by models 3 and 4 for different values of n, are also depicted. In Figs. 6 to 8 the behavior of the strength can be divided into three ranges. In the first range, of low values of the filler content, it seems that fracture occurs at a finite number of individual inclusions, so that the strength can be related to the quality of the adhesion between the matrix and filler, while the crack pinning effect is not predominant. In the second range it seems that fracture occurs at a finite number of

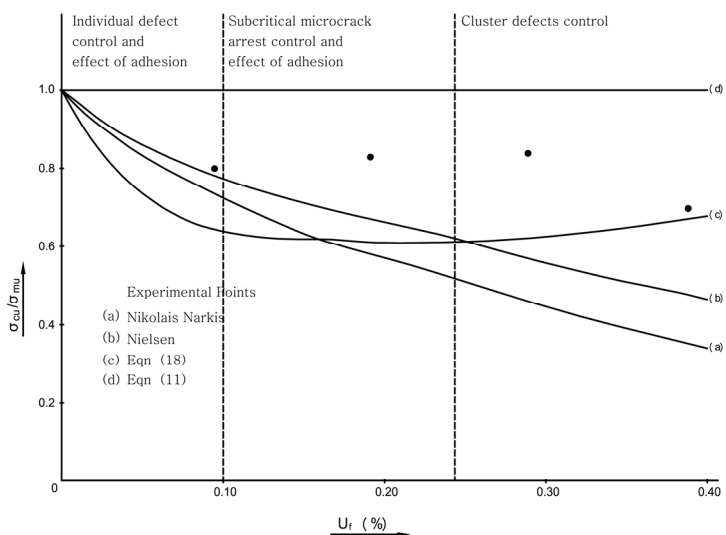

Fig. 6. *Ratio* σ_{cu}/σ_{mu} *as a function of the volume fraction* u_f *in resin/iron particulate composites*

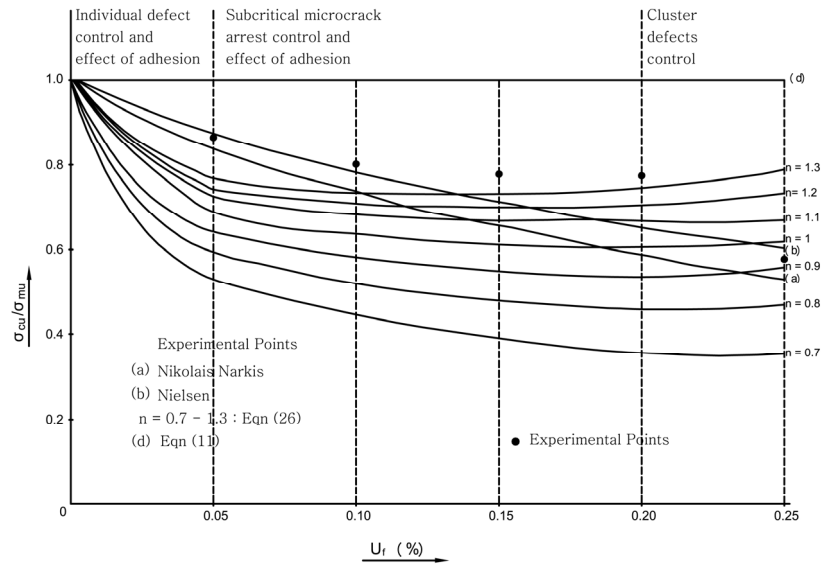

Fig. 7. *Ratio σ_{cu}/σ_{mu} as a function of the volume fraction u_f in resin/iron particulate composites*

individual inclusions, and a combination of the quality of the adhesion between the matrix and filler with the crack pinning effect are predominant. In the third range it seems that fracture occurs in agglomerations-clusters. In Figs. 6 and 7 one can observe that inside the second range, the average value of the strength derived by the Models 1 and 2, approximates the experimental results. It seems that the quality of the adhesion between the matrix and filler corresponds to a mean value between the values of the adhesion qualities which are provided by the Models 1 and 2. This second region is characterized by an equilibrated-constant value of the strength given by the experimental results, which can be interpreted by the presence of adhesion and the crack pinning effect (crack arrest). It can be observed that this equilibrated-constant value of the strength results from Eqs. (11) and (18) and not from Eqs. (33) and (34).

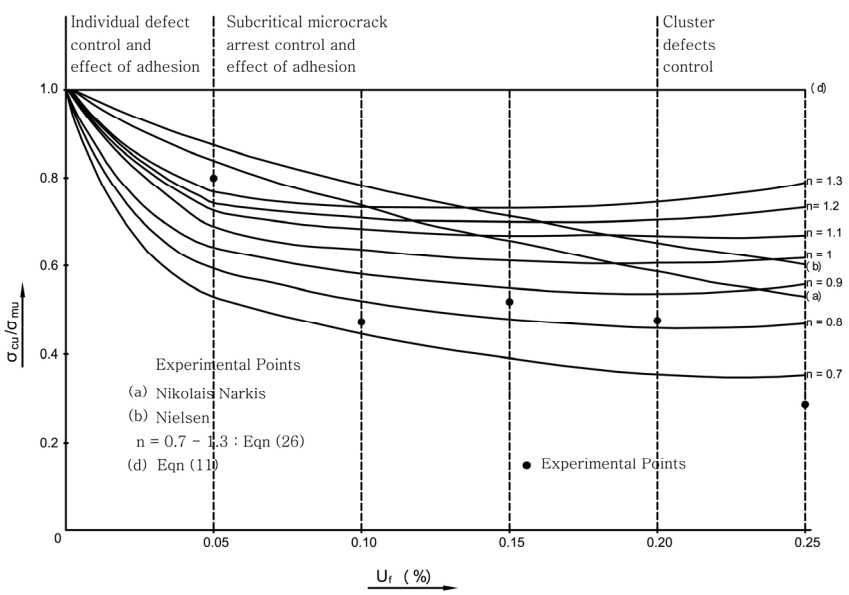

Fig. 8. *Ratio σ_{cu}/σ_{mu} as a function of the volume fraction u_f in resin/iron particulate composites*

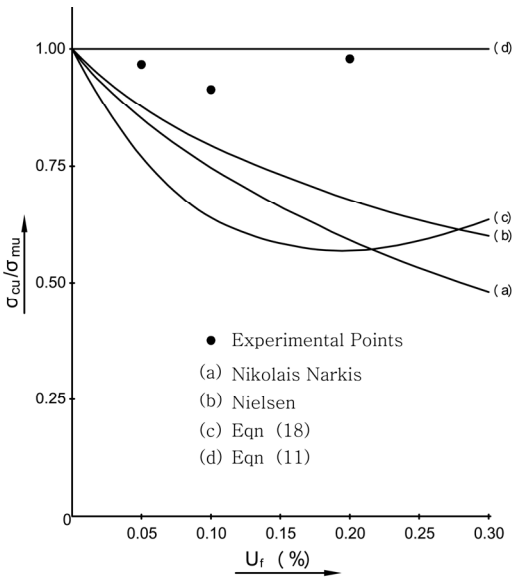

Fig. 9. *Ratio σ_{cu}/σ_{mu} as a function of the volume fraction u_f in resin/SiC particulate composites*

The values of the experimental points in Fig. 8 are lower compared to the values of the experimental points in Figs. 6 and 7. This can be interpreted with the remark that probably there is an inhomogeneous distribution of the filler in the volume of the matrix and the strength can be evaluated using Model 4 with n<1. Actually, Model 4 seems that corresponds to a single quality of the adhesion between matrix and filler, but it gives different values of the strength, depending on *n*. Thus one can say that this model can be characterized as an idealized model corresponding to different low and intermediate qualities of the adhesion. The local stress concentration factors of Model 4 are given in Appendix 2.

The experimental results shown in Fig. 9 can be interpreted considering an "optimal" combination of the quality of the adhesion between the filler and matrix, and the crack pinning effect since there can be a competing effect between a high adhesion quality and a low effect of the crack arrest, or between an intermediate adhesion quality and a high effect of the crack arrest [13]. It can be seen that in this case the experimental results are close to the theoretical results provided by Models 1 and 3. From the experimental results shown in Fig. 9 it can be concluded that agglomerations do not exist in the specimens.

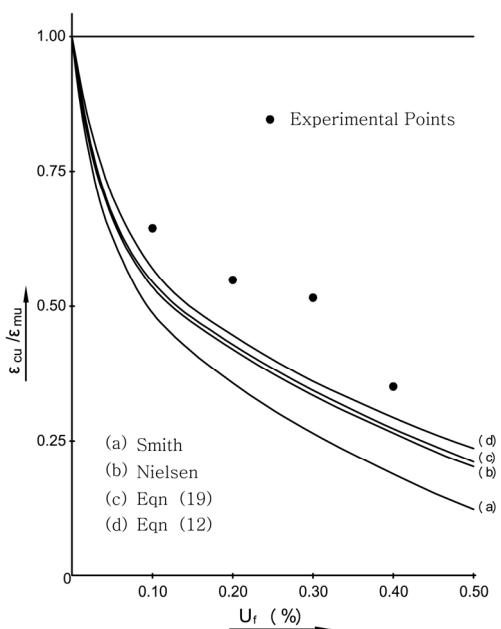

Fig. 10. *Ratio $\varepsilon_{cu}/\varepsilon_{mu}$ as a function of the volume fraction u_f in resin/iron particulate composites*

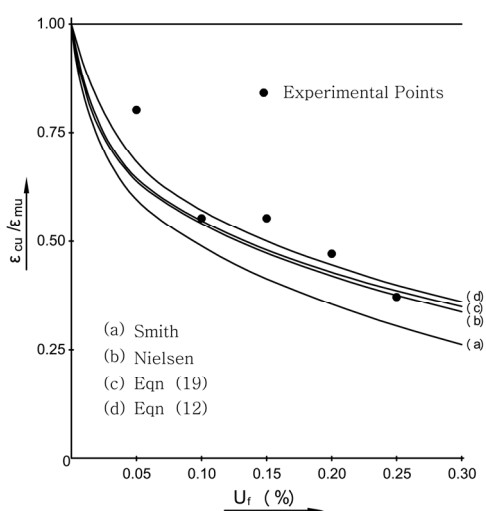

Fig. 11. *Ratio $\varepsilon_{cu}/\varepsilon_{mu}$ as a function of the volume fraction u_f in resin/iron particulate composites*

It can be noticed that the theoretical results of the stresses furnished by Eqs. (33) and (34) correspond to the case that when there is no adhesion between the matrix and filler, which implies that stresses are not transferred to the inclusion. The deviation of these theoretical results from those predicted by the presented models can be explained by the fact that in the presented models there is adhesion between the matrix and filler and thus stresses are transferred to the inclusion. This can explain clearly why in the presented models the strength is not a decreasing function of u_f as in the case of Eqs. (33) and (34).

In Figs. 10 to 12 the ratio of the fracture strain of the composite to the fracture strain of the matrix is plotted, versus the filler volume fracture in resin/iron composites (Figs. 10 and 11) and in resin/SiC particulate composites (Fig. 12). In the same figures the theoretical results given by Eqs. (A3) and (A4) (Appendix 1) as well as those given by the used models are also presented.

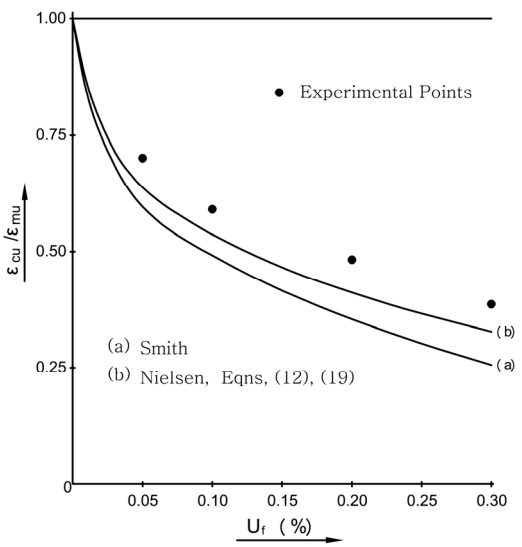

Fig. 12. *Ratio $\varepsilon_{cu}/\varepsilon_{mu}$ as a function of the volume fraction u_f in resin/SiC particulate composites*

In Figs. 10 to 12 the ratio of the fracture strain of the composite to the fracture strain of the matrix is plotted, versus the filler volume fracture in resin/iron composites (Figs. 10 and 11) and in resin/SiC particulate composites (Fig. 12). In the same figures the theoretical results given by Eqs. (35) and (36) (Appendix 1) as well as those given by the used models are also presented. From these figures it can be verified that the above theoretical results are very close. This can be explained by taking into account the fact that in all those equations it was assumed that there is adhesion between the matrix and filler. In [1] Nielsen mentions that in the case of no adhesion, the fracture strain takes higher values than those provided by Eq. (35). In Figs. 10 and 11 it can be seen that the experimental results are approximated closer by the theoretical results provided by Model (1) than by the results of the other models. The high values of strength in Fig. (10) can be explained by the homogeneous distribution of the filler in the volume of the matrix (Model (4), n>1) and probably by viscoelastic and plastic phenomena taking place in the matrix. As can be easily verified from Eqs. (24) and (27), the fracture strain in Models 3 and 4 is a decreasing function of n (the same holds in the case of strength). In Fig. 12 the theoretical results given by Eqs. (12), (19) and (35) coincide. This is due to the high value of $m = E_f / E_m$. It is remarkable to notice that although Models 1 and 2 correspond to different adhesion qualities as far as the strength is concerned, however both models give almost the same values for the fracture strain. This can be explained by taking into account that the values of the elastic moduli, provided by each of the above models, are different.

The presented procedure for the evaluation of the strength and the fracture strain in both models is in agreement with Nielsen's theory in which the strength is given by

$$\sigma_{cu} = \varepsilon_{cu} E_c , \tag{30}$$

where ε_{cu} is given by Eq. (35) (Appendix 1). Thus, since the predicted strains by the presented models are close to the strains provided by Eqs. (35), (11) and (18), as well as Eqs. (30) and (35) give the same values of the strength respectively.

4 MICROFAILURE EFFECTS

In Fig. 9 the curve of the ultimate stress behavior versus the variation of the volume fraction for Epoxy-matrix-SiC particles is shown. By comparison with Figs. 6 to 8 referring to the case of Fe-particles, an overall shift of the first curve to higher values can be deduced, a fact which means an increasing microcrack-pinning-arrest effect on the critical crack propagation in

the given composite. In [13] a detailed explanation of such effects by means of an elastic-small scale yielding microfracture-fracture toughness modeling approach, is presented. In [13] it was shown that similar ultimate stress behavior as observed in the above figures, can be explained by taking into consideration the degree of inhomogeneity expressed by some structural parameters such as the particle (inclusion) size as well as the interinclusion spacing. In the light of the mentioned reference it can be argued that the above observed shift may be also attributed to the difference of the SiC particle average size of ~75 μm compared to Fe-particle size of ~150 μm. Furthermore, from the well-known relation for the fracture toughness $K_c = \sigma_f \sqrt{\pi a_0}$ taken as a constant material parameter, it is easy to deduce that an increase (decrease) of the defect (inclusion/particle) size a_0, can lead to a decrease in the fracture stress σ_f. Therefore, for the same volume fraction and adhesion strength, the reduced particle size of SiC can also lead to a relative increase in the fracture (ultimate) stress of the composite and in this way to the observed shift to higher values compared to Fe-particle composite. At the same time the mechanism of microcrack-pinning and/or arrest can play a competing role. This means that for the same volume fraction and adhesion strength, the probability for a microcrack to become pinned and/or arrested around a particle is higher for a composite with finer dispersed particles (SiC), where the effective interinclusion spacing is smaller compared to Fe-composite, where the effective interinclusion spacing is greater.

5 STRENGTH AND ULTRASOUNDS

It is known that the strength is related with the hardness predicted by Brinel's method. The existing relation is:

$$\sigma = k \cdot BHN_{30}, \tag{31}$$

where *BHN* is Brinel's hardness and *k* is a constant of the material. The index 30 corresponds to the relation:

$$\lambda = 30 = \frac{P}{D^2}, \tag{32}$$

where *P* is the applied load on the specimen and *D* is the diameter of the penetrator.

It is also known that the hardness can be obtained by means of ultrasonic measurements. The constant *k* of Eq. (31) can be determined by this method.

An alternative way to estimate the strength of particulate composites is to use Eqs. (30) and (35) in which the value of the elastic modulus can be measured using ultrasounds.

This study presents two models for the evaluation of the strength which can be used for a comparison to the strength evaluated by ultrasonic measurements.

6 CONCLUSIONS

1. The strength evaluated by Model 1 is independent of the filler volume fraction and equal to the strength of the matrix. This value of strength compared to experimental results is found to be close to the strength of treated particles and gives an upper bound of the strength of particulate composites predicted by cube-within-cube models. The model is characterized as corresponding to perfect adhesion quality.
2. Comparing the strength obtained by Model 2 to experimental results, it is found to be close to the lower values of the strength of untreated particles. Thus, the model is characterized as corresponding to low adhesion quality. The strength derived by Model 2 does not give a lower bound of the strength of particulate composites.
3. The strength predicted by the presented procedure is in agreement to the strength predicted by Nielsen's theory when there is adhesion between matrix and filler.
4. In Model 2, when an initial failure takes place in the matrix, a local stress concentration factor is assumed by means of which the failure in the whole composite is considered.
5. Although Models 1 and 2 correspond to different adhesion qualities as far as the strength is concerned, however they provide almost the same values of the fracture strain.
6. When there are not agglomerations, the adhesion quality and the crack pinning effect seem to be predominant in the fracture behavior of the composite. As it arises from Models 3 and 4 and the experimental results, inhomogeneities in the composite influence the values of the strength and the fracture strain.

7 APPENDIX 1

Equations of the strength used for comparison:

1) Nielsen's equation (no adhesion) [1]

$$\sigma_{cu} = \sigma_{mu}(1-u_f^{2/3})\cdot k\,, \tag{33}$$

where k is a stress concentration factor.

2) Nikolais and Narkis equation (no adhesion) [10] and [11]

$$\sigma_{cu} = \sigma_{mu}(1-1{,}21\,u_f^{2/3})\,. \tag{34}$$

3) Nielsen's equation for fracture strain [1]

$$\varepsilon_{cu} = \varepsilon_{mu}(1-u_f^{1/3})\,. \tag{35}$$

4) Smith's equation for fracture strain [12]

$$\varepsilon_{cu} = \varepsilon_{mu}(1-1.106\,u_f^{1/3})\,. \tag{36}$$

APPENDIX 2

Values of the Local Stress Concentration Factor in Model 4:

1) In the case of Model 4 failure of the component (2) causes failure of the whole composite in which the local concentration factor K is given by:

$$\sigma_3 = K\left[\sigma_{mu}\frac{m(n-u_f^{1/3})+u_f^{1/3}}{m\,n}+\sigma_{mu}\frac{u_f^{2/3}}{n^{-1}u_f^{2/3}}\right]\geq\sigma_{mn} \tag{37}$$

2) In Model 2 the values of the concentration factor K in epoxy/iron composites are given in the following Table 2, for different values of n and u_f.

As it turns out, the values of the concentration factor, when $n < 1$, are not too high, if one considers that at a circular hole in an infinite plate the concentration factor is $n = 3$ [14].

8 REFERENCES

[1] Nielsen, L.E. (1966). Simple theory of stress-strain properties of filled polymers. *Journal of Applied Polymer Science*, vol. 10, p. 97-103.

[2] Ahmed, S., Jones, F.R. (1990). A review of particulate reinforcement theories for polymer composites. *Journal of Materials Science*, vol. 25, no. 12, p. 4933-4942.

[3] Moloney, A.C., Kausch, H.H., Kaiser, T., Beer, H.R. (1987). Review. Parameters determining the strength and toughness of particulate filled epoxide resins. *Journal of Materials Science*, vol. 22, p. 381-393.

[4] Spanoudakis, J., Young R.J. (1984). Crack propagation in a glass particle-filled epoxy resin, Part1: Effect of particle volume fraction and size, *Journal of Materials Science*, vol. 19, p. 473-486.

[5] Spanoudakis, J., Young, R.J. (1984). Crack propagation in a glass particle-filled epoxy resin, Part2: Effect of particle-matrix adhesion, *Journal of Materials Science*, vol. 19, p. 487-496.

[6] Kinloch, A.J., Maxwell, D.L., Young, R.J. (1985). The fracture of hybrid-particulate composites. *Journal of Materials Science*, vol. 20, p. 4169-4184.

[7] Paul, B. (1960). Prediction of elastic constants of multiphase materials. *Transactions of the Metallurgical Society of AIME,* vol. 218, p. 36-41.

Table 2. *The values of the concentration factor K*

n	u_f				
	0.05	0.10	0.15	0.20	0.25
1.3	1.07	0.964			
1.2	1.12	1.03	0.93		
1.1	1.18	1.12	1.07	0.93	
0.9	1.35	1.36	1.31	1.23	1.13
0.8	1.50	1.57	1.57	1.52	1.45
0.7	1.70	1.90	2.00	2.03	2.00

[8] Ishai, O., Cohen, L.J. (1967). Elastic properties of filled and porous epoxy composites. *International Journal of Mechanical Sciences*, vol. 9, no. 8, p. 539-546.

[9] Prassianakis, I.N., Kourkoulis, S.K. (1999). *Experimental Strength of Materials* Symmetria Editions, Athens.

[10] Nikolais, L., Mashelkar, R.A. (1976). The strength of polymer composites containing spherical fillers. *Journal of Applied Polymer Science*, vol. 20, p. 561-563.

[11] Narkis, J. (1975). Crazing in glassy polymers: studies on polymer-glass bead composites, *Polymer Engineering and Science,* vol. 15, no. 4, p. 316-320.

[12] Smith, T.L. (1961). Volume changes and dewetting in glass bead-polyvinyl chloride elastometric composites under large deformations. *Rubber Chemistry and Technology*, vol. 34, p. 125-140.

[13] Kytopoulos, V. Sideridis, N.E., Bourkas, G. (2003). A study of some thermomechanical and fractural properties of particle reinforced polymer composites and SEM-aided microfailure approach of certain fracture parameters, *Journal of Reinforced Plastics and Composites*. vol. 22, no. 17, p. 1547-1587.

[14] Andrianopoulos Kyriazi N.E., Liakopoulos, K. (1988). *Experimental Strength of Materials*. Simeon Editions, Athens.